ACS NANO
Cite This: ACS Nano XXXX, XXX, XXX−XXX
www.acsnano.org

ARTICLE

Contact-Electrification between Two Identical Materials: Curvature Effect

Cheng Xu,[†,‡,§,∥] Binbin Zhang,[§,∥] Aurelia Chi Wang,[§,∥] Haiyang Zou,[§] Guanlin Liu,[§] Wenbo Ding,[§] Changsheng Wu,[§] Ming Ma,[‡] Peizhong Feng,[‡] Zhiqun Lin,[§] and Zhong Lin Wang*[,†,§,⊥]

[†]Beijing Institute of Nanoenergy and Nanosystems, Chinese Academy of Sciences, Beijing 100083, China
[‡]School of Materials Science and Engineering, China University of Mining and Technology, Xuzhou 221116, China
[§]School of Materials Science and Engineering, Georgia Institute of Technology, Atlanta, Georgia 30332-0245, United States
[⊥]School of Nanoscience and Technology, University of Chinese Academy of Sciences, Beijing 100049, China

Supporting Information

ABSTRACT: It is known that contact-electrification (or triboelectrification) usually occurs between two different materials, which could be explained by several models for different materials systems (*Adv. Mater.* 2018, *30*, 1706790; *Adv. Mater.* 2018, *30*, 1803968). But contact between two pieces of the chemically same material could also result in electrostatic charges, although the charge density is rather low, which is hard to understand from a physics point of view. In this paper, by preparing a contact-separation mode triboelectric nanogenerator using two pieces of an identical material, the direction of charge transfer during contact-electrification is studied regarding its dependence on curvatures of the sample surfaces. For materials such as polytetrafluoroethylene, fluorinated ethylene propylene, Kapton, polyester, and nylon, the positive curvature surfaces are net negatively charged, while the negative curvature surfaces tend to be net positively charged. Further verification of the above-mentioned trends was obtained under vacuum (∼1 Pa) and higher temperature (≤358 K) conditions. Based on the received data acquired for gentle contacting cases, we propose a curvature-dependent charge transfer model by introducing curvature-induced energy shifts of the surface states. However, this model is subject to be revised if the mutual contact mode turns into a sliding mode or more complicated hard-pressed contact mode, in which a rigorous contact between the two pieces of the same material could result in nanoscale damage/fracture and possible species transfer. Our study provides a primitive step toward understanding the basics of contact-electrification.

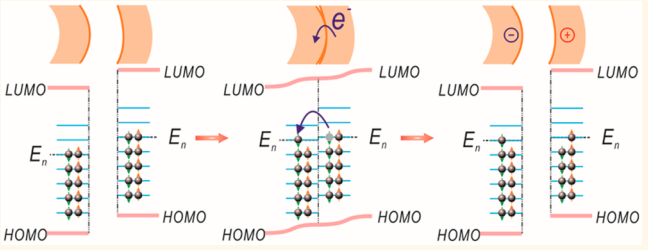

KEYWORDS: *contact-electrification, triboelectrification, triboelectric nanogenerator, curvature, identical material, surface states*

It is well known that a contact-separation interaction between two dissimilar materials enables each material surface to accumulate an equivalent amount of net opposite charges, that is, the occurrence of contact-electrification (CE) (or triboelectrification). Generally speaking, CE between distinct materials is attributed to the work function or contact potential difference[1,2] and can be attributed to the surface states model or electron-potential well model.[3−7] However, CE can also occur between chemically identical materials that have the same contact potential. For instance, it emerges in some natural phenomena such as volcanic plumes,[8] sand storms,[9] and dust devils,[10] and even in industrial processes involving small particles.[11] With regard to CE between homologous materials, there is still no reasonable consensus in interpreting and explaining its mechanism. For example, Herry proposed that charge transfer was due to a temperature difference caused by asymmetric rubbing of two surfaces.[12] Lowell and Truscott showed that charge transfer occurred during asymmetric rubbing even though temperature and other physical properties remained exactly the same for the two surfaces.[13] They proposed that CE was attributed to nonequilibrium electron distributions and transfer of electrons between localized states in insulators. On the other hand, Baytekin *et al.* assumed that random "mosaics" of oppositely charged regions on each surface led to CE between identical materials, and these charged mosaics were related to the transfer of charged material patches.[14]

It is noteworthy that CE is a rather sophisticated and complex process since diverse relative motions are likely to occur between the two contacting materials. To simplify, these relative motions can be defined as sliding (or rubbing) and

Received: November 8, 2018
Accepted: February 1, 2019
Published: February 1, 2019

DOI: 10.1021/acsnano.8b08533
ACS Nano XXXX, XXX, XXX−XXX

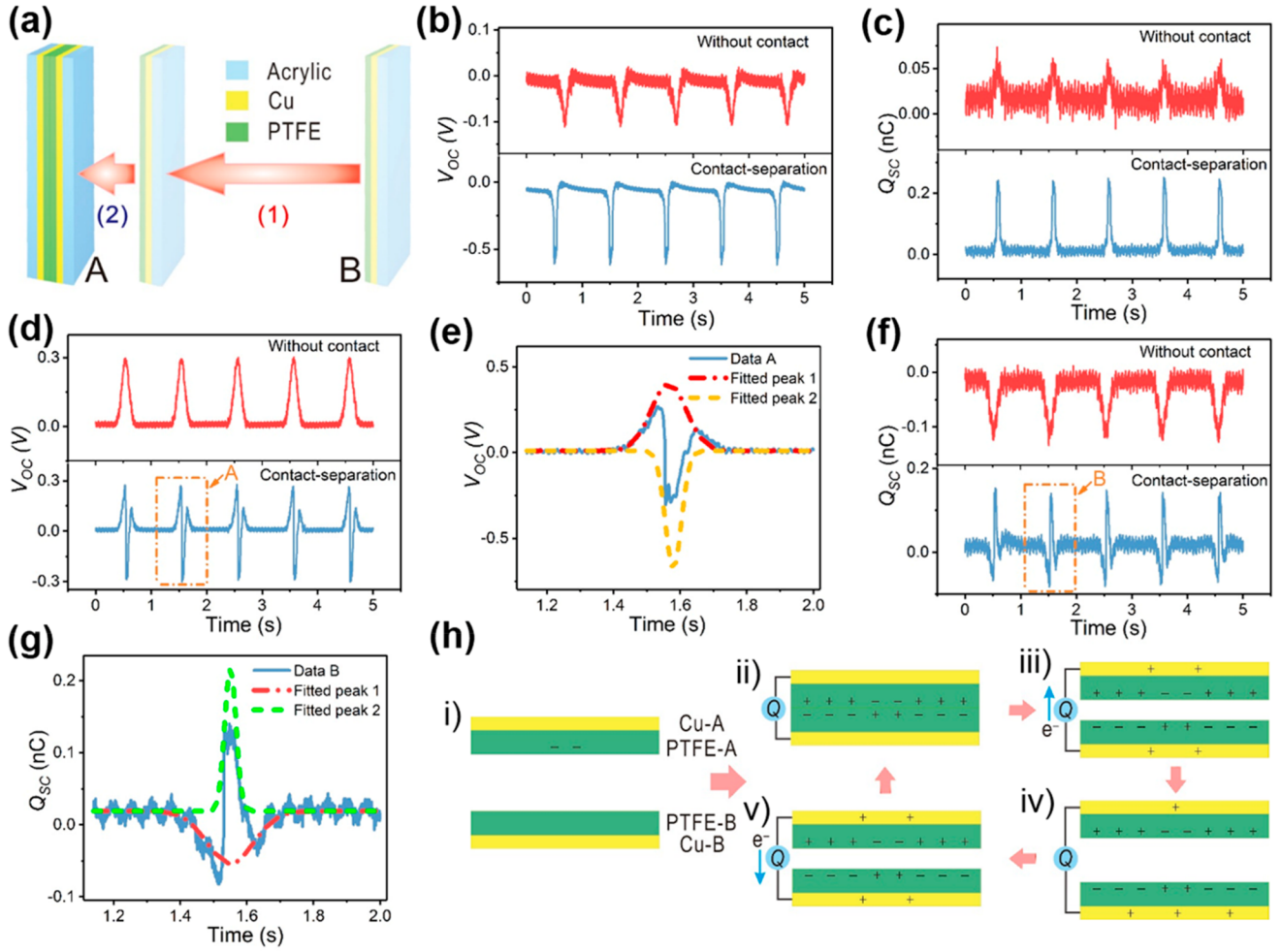

Figure 1. Effect of initial charges on CE between identical materials. (a) Diagram of the two phases during the operation of the TENG. (b, c) Typical V_{OC} and Q_{SC} of the TENG with few initial negative charges on the surface of PTFE-B. (d–g) Typical V_{OC} and Q_{SC} of the TENG with few initial negative charges on the surface of PTFE-A. (h) Working principle of the TENG with few initial negative charges on the surface of PTFE-A.

contact-separation. There is no doubt that sliding is liable to cause surface damage to materials, especially polymers. The close relation between the surface properties of polymers and CE results in surface damage significantly affecting the ultimate electrical outcome. Moreover, surface damage causes less material transfer to dominate the CE process, altering the authentic direction of charge transfer. However, provided that contact-separation with a gentle force is applied, surface damage can be avoided to some extent, likely reaching reliable conclusions in analyzing CE. Fortunately, the recently invented triboelectric nanogenerator (TENG) can be used to perform precise, real-time quantitative measurements of surface charges and thus produce power for harvesting broad-range energy sources in the ambient environment.[15−19] In particular, the TENG has various working modes, including a contact-separation mode, and is capable of fine-tuning the magnitude of exerted forces,[20−23] which provides an ideal platform for in-depth research on the CE mechanism between identical materials. We have previously studied the CE of two dissimilar materials and proposed related models for different materials systems.[7,24,25]

In this paper, we designed and prepared a TENG using two pieces of a chemically identical material but with surfaces of different macroscale shapes or curvatures and investigated the direction of charge transfer in real time *via* the TENG operated on the contact-separation mode. It was found that a convex surface with positive curvature was prone to be negatively charged, while a concave surface with negative curvature was inclined to be positively charged. In addition, an increase of applied pressure/force was likely to lead to a reversal of charge transfer direction between the two pieces. Moreover, further verification on the above-mentioned charge trends between identical materials was conducted under vacuum and high temperatures. Based on the research findings, a surface states model was proposed to explain the CE mechanism between identical materials.

RESULTS AND DISCUSSION

Polytetrafluoroethylene (PTFE) films were utilized as the tribomaterial of the TENG, in which the left-hand PTFE (PTFE-A) was fixed and the right-hand PTFE (PTFE-B) approached and contacted PTFE-A (Figure S1). If the PTFE-A surface has many initial negative charges before the TENG operation, the results show a positive open circuit voltage (V_{OC}) and a negative short circuit transfer charge (Q_{SC}). Here, the initial negative charges on PTFE-A were introduced by rubbing it with a Cu foil. Since PTFE-B is the reference to evaluate PTFE-A, a negative sign of Q_{SC} indicates more

DOI: 10.1021/acsnano.8b08533
ACS Nano XXXX, XXX, XXX−XXX

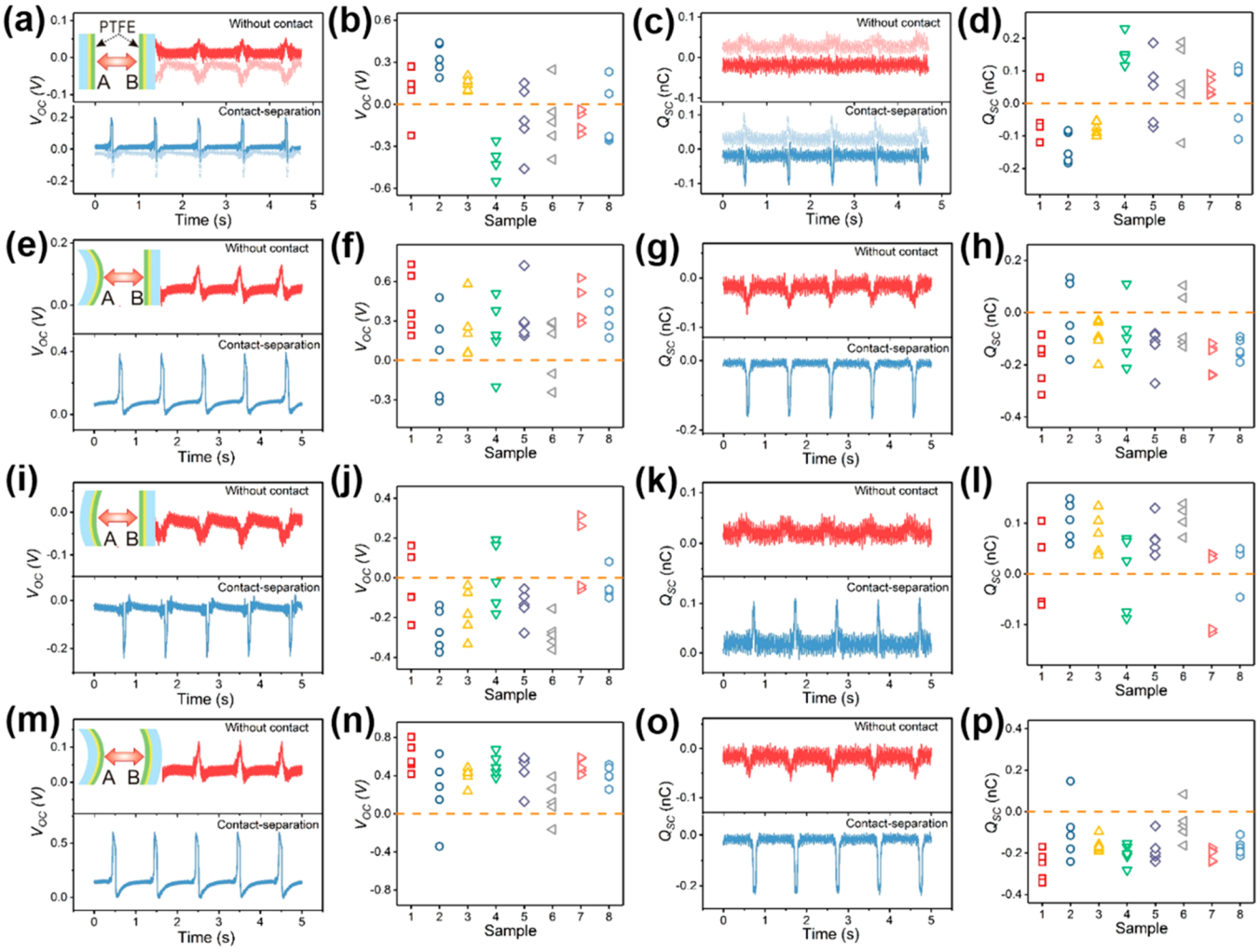

Figure 2. Properties of the PTFE TENG with surfaces of different shapes. (a–d) V_{OC} and Q_{SC} of the TENG with two flat surfaces. (e–h) V_{OC} and Q_{SC} of the TENG with a convex surface (curvature of 0.20 cm^{-1}) and a flat surface. (i–l) V_{OC} and Q_{SC} of the TENG with a concave surface (curvature of −0.07 cm^{-1}) and a flat surface. (m–p) V_{OC} and Q_{SC} of the TENG with a convex surface (curvature of 0.20 cm^{-1}) and a concave surface (curvature of −0.07 cm^{-1}). The applied force during the contact-separation CE process is 2 ± 0.5 N.

negative charges on PTFE-A than those on PTFE-B. However, it is noteworthy that since PTFE-A carries a lot of negative charges prior to the measurement, it is unclear if the negative charge transfer from PTFE-B to PTFE-A or *vice versa* is in accordance with the sign of Q_{SC}. Conversely, provided that more initial negative charges were introduced to the PTFE-B surface with the friction of Cu foil, the results revealed a negative V_{OC} and a positive Q_{SC}, indicating more positive charges on PTFE-A or more negative charges on PTFE-B. These aforementioned measurements cannot be used to interpret the actual direction of charge transfer in CE, but only reflect the ultimate charge difference of the material surfaces.[26] Discharge is therefore conducted on both the acrylic substrates and tribomaterials of the TENG prior to measurements to avoid the detrimental effect of the initial residual charges on the surfaces. Meanwhile, the operation of the TENG is categorized into two phases, as shown in Figure 1a. The moment when PTFE-B moves to a very close but inaccessible position with regard to PTFE-A is phase 1, in which the generated V_{OC} and Q_{SC} mainly reflect the induction effect of initial residual charges on the surfaces, but no charge transfer occurs since there is no firm contact between the two surfaces. Once the contact occurs between PTFE-B and PTFE-A (phase 2), the generated V_{OC} and Q_{SC} reflect the combined influence of initial residual charges and transferred charges in CE. Figure 1b,c demonstrate that there are more positive charges on PTFE-A than on PTFE-B before contact; that is, PTFE-B is negatively charged with less electricity after discharging. After contact, the positive charges on PTFE-A increase; in other words, the electrons flow from PTFE-A to PTFE-B. Due to the slight differences of each discharge treatment, another condition of Figure 1d–g is likely to occur. Under that condition, PTFE-A is negatively charged with more electrons than PTFE-B. However, the peak shape of either V_{OC} or Q_{SC} after contact becomes irregular; that is, the peak reverses at the maximum value. Figure 1e,g shows the fitted peaks of peaks A and B in Figure 1d,f, suggesting that the shapes of both peaks are attributed to the superposition of two peaks. The direction of one peak is in accordance with that prior to contact, resulting from the induction of initial charges. Another peak is a reverse one, relying on charge transfer in CE. Here, the negative sign of V_{OC} and positive sign of Q_{SC} indicate more positive charges on PTFE-A, which means the electrons transfer from PTFE-A to PTFE-B, similar to that shown in Figure 1b,c. Figure 1h illustrates the working principle of the TENG with few initial negative charges on the surface of

DOI: 10.1021/acsnano.8b08533
ACS Nano XXXX, XXX, XXX–XXX

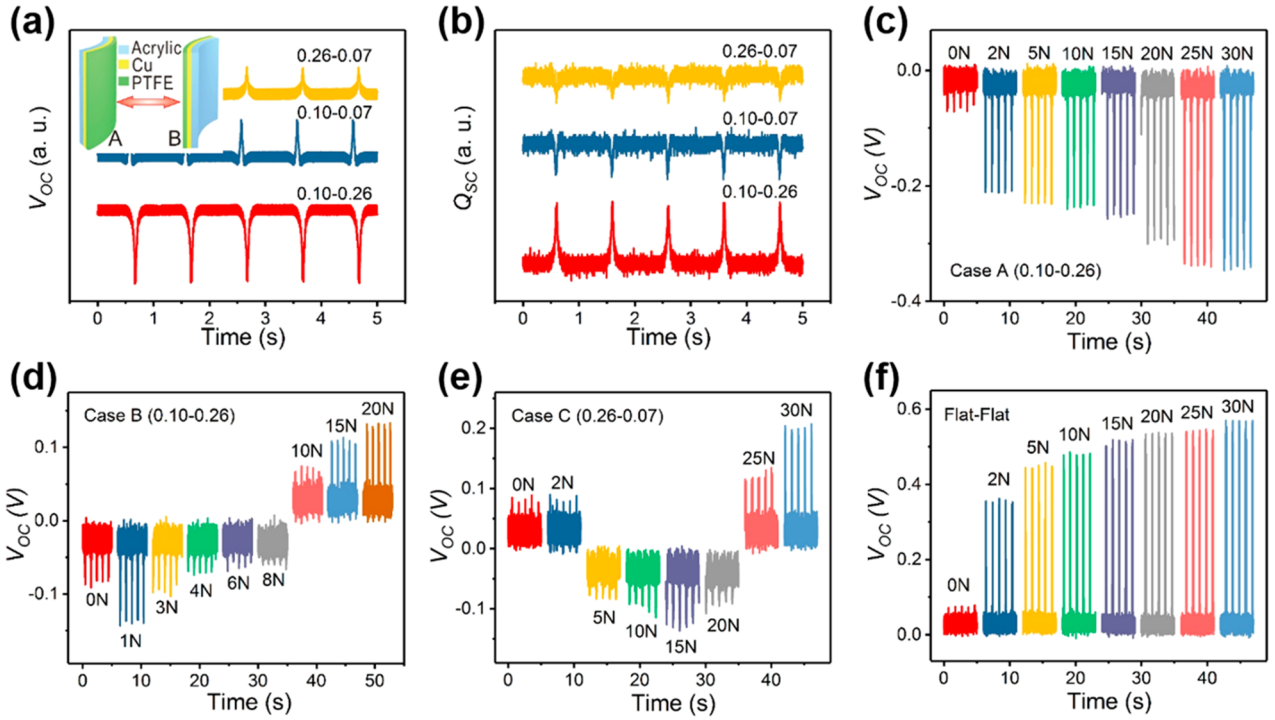

Figure 3. Effect of applied forces on the properties of a PTFE TENG. (a, b) Typical V_{OC} and Q_{SC} of the TENG with convex surfaces of different curvatures. (c, d) V_{OC} of the TENG with a surface curvature of 0.10 and 0.26 cm^{-1}. (e) V_{OC} of the TENG with surface curvatures of 0.26 and 0.07 cm^{-1}. (f) V_{OC} of the TENG with two flat surfaces.

PTFE-A. When the two PTFE films come into contact, opposite triboelectric charges will be generated on the surfaces. These charges are partly induced by initial residual negative charges on PTFE-A, yielding equivalent positive charges on PTFE-B. Another portion of the negative charges on PTFE-A and equivalent positive charges on PTFE-B are generated because of CE. Overall, PTFE-A is positively charged and PTFE-B is negatively charged. Upon release, the two oppositely charged surfaces start to separate from each other, inducing a potential difference between the two Cu electrodes. This potential difference will drive electrons to flow from the Cu-B electrode to Cu-A electrode. When the separation between the two surfaces reaches a maximum, almost all of the positive charges on the Cu-A electrode will be neutralized. Subsequently, when the PTFE films approach each other again, the reversed potential difference between the two electrodes will be built up, which leads to a back flow of all of the transferred electrons from the Cu-A electrode to the Cu-B electrode. Figure 1 also reveals that, even though complete elimination of the initial charges is impossible, the charge reduction can also assist in the assessment of actual direction of charge transfer in CE to some extent. Based on these findings, initial charge elimination is conducted prior to measurement in the following experiment.

What are depicted in Figure 2 are the performances of PTFE TENGs with surfaces of diverse shapes. Figure 2a,c are the typical V_{OC} and Q_{SC} of the TENG with two flat surfaces. Eight sets of samples are assessed five times for each in Figure 2b,d. Accordingly, no apparent tendency of the direction of charge transfer is shown with two flat films; in other words, the transfer probability of the electrons from PTFE-A to PTFE-B or *vice versa* is around half to half. It must be noted that since it is necessary to remove the samples, rinse them with anhydrous ethanol to discharge after each test, and continue a new test after reinstallment, the surface contact position of the samples likely differs each time. This may lead to a reversal in direction of charge transfer in CE at different times using the same set of samples. Therefore, we confirmed the consistency in surface contact position at each time and reassessed sample 5 in Figure 2b,d ten times (Figure S2). It is shown that the direction of charge transfer is the same even though the transferred amount of charges differs each time. This is due to the so-called "memory effect".[27] Therefore, it is believed that there is a certain regularity of direction of charge transfer for CE between identical materials, which may be relevant to the surface status. Figure 2e–h is the V_{OC} and Q_{SC} of the TENG with a convex surface of positive curvature and a flat surface. It is shown that the convex PTFE film is negatively charged in most cases, which indicates that it gains electrons more readily than the flat film. Figure 2i–l is the V_{OC} and Q_{SC} of the TENG with a concave surface of negative curvature and a flat surface. The concave PTFE films are positively charged in most cases, which means they are less likely to gain electrons than flat films. Figure 2m–p is the V_{OC} and Q_{SC} of the TENG with a convex surface and a concave surface. To improve the quality of contact-separation operation and avoid unintentional contact in other modes, such as sliding, the curvature of the convex PTFE film is set as 0.20 cm^{-1} and that of the concave PTFE film is set as −0.07 cm^{-1}. In addition, the V_{OC} and Q_{SC} of the TENG that had the PTFE films with opposite but the same magnitude of curvatures as 0.20 cm^{-1} and −0.20 cm^{-1} were also measured (Figure S3). These convex–concave pairings reveal that the convex PTFE film is more prone to acquire electrons than the concave film. Figure 2e–p indicate that a surface of larger curvature gains negative charges more easily, which is consistent with the V_{OC} and Q_{SC} results of the contact-separation mode fluorinated ethylene propylene (FEP) TENG, Kapton TENG, polyester TENG, and nylon TENG

DOI: 10.1021/acsnano.8b08533
ACS Nano XXXX, XXX, XXX–XXX

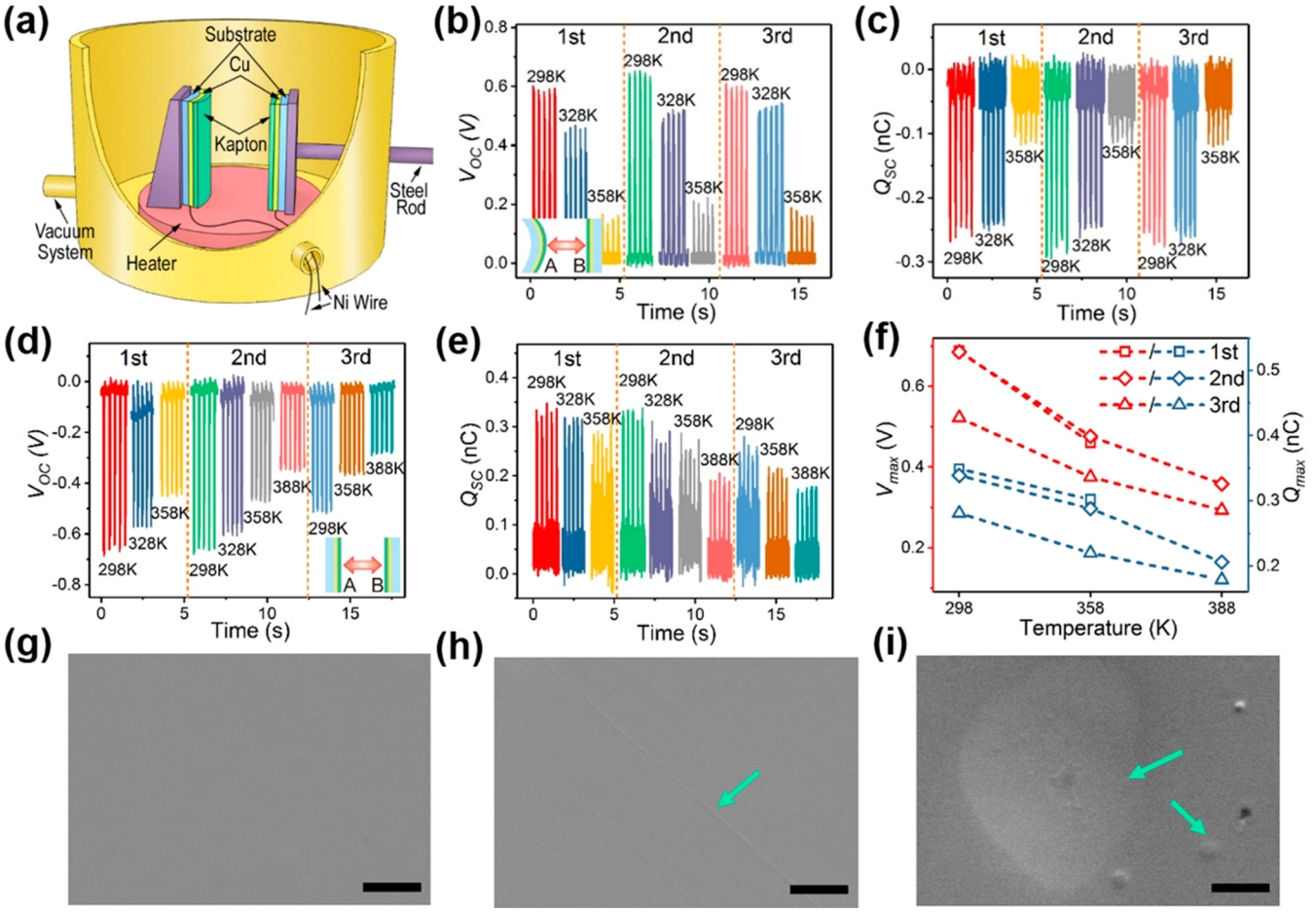

Figure 4. Temperature effects on the properties of Kapton TENG. (a) Setup of the vacuum chamber and high-temperature test platform. (b, c) V_{OC} and Q_{SC} of the TENG with a convex surface (curvature of 0.20 cm^{-1}) and a flat surface at different temperatures. (d, e) V_{OC} and Q_{SC} of the TENG with two flat surfaces at different temperatures. (f) Maximum V_{OC} and Q_{SC} of the TENG with two flat surfaces at different temperatures. (g–i) SEM images of the Kapton surface before and after 358 and 388 K measurement, respectively. The scale bar is 10 μm.

with convex–flat, concave–flat, and convex–concave surfaces (Figures S4–7).

Figure 3a,b are the typical V_{OC} and Q_{SC} of the PTFE TENG with surfaces of different positive curvatures. In addition, the measurement is conducted on five sets of samples five times each, in which the surface curvatures of the TENG are 0.26 and 0.07 cm^{-1} (Figure S8). These results coincide with those in Figure 2, suggesting that larger curvature leads to a more negatively charged surface. It is intriguing that similar findings were shown in studies on CE of particles; that is, a particle with a smaller radius was more likely to be negatively charged when contacted with another chemically identical larger particle.[28−30]

Illustrated in Figure 3c,d is the effect of applied forces on the performance of the TENG with a surface curvature of 0.10 and 0.26 cm^{-1}. Because it is difficult to precisely measure the Q_{SC} when a miniscule contact force is applied, only the variation of V_{OC} with increasing force is investigated to estimate the direction of charge transfer. Figure 3c shares the same findings as previous results, demonstrating that the increased applied force results in a gradual increase of V_{OC}.[31,32] This is mainly attributed to the fact that the increased force enlarges the contact area between the two surfaces of the TENG. However, it is interesting that the increased applied force also results in another situation as shown in Figure 3d, which has not been previously reported in the TENG studies. The increase of applied force to 3 N inversely leads to the reduction of V_{OC}, and the further increase of the force to 10 N results in a complete reversal of V_{OC} (*i.e.*, the direction of charge transfer reverses). What is more, the CE of the TENG with surface curvatures of 0.26 and 0.07 cm^{-1} creates a more complicated case; that is, two separated reversals in V_{OC} occur with the increase of applied force (Figure 3e). The V_{OC} variation along with a gradual increase of the applied forces in CE of the TENG with two flat surfaces is measured to compare the results (Figure 3f). It indicates that V_{OC} gradually increases with the increase of the applied forces in most cases. The above findings suggest that the CE of two convex surfaces is prone to reverse the direction of charge transfer as applied force increases, while flat surfaces undergoing CE of increasing force do not tend to reverse the direction of charge transfer. Here, as for the mutual contact between two convex surfaces, the increase of applied forces is more likely to change the mode of relative motions rather than merely an increase in contact area, such as the transformation from contact-separation mode to sliding mode. The continuous increase of applied forces may generate some surface damage and even lead to material transfer. All of the above reasons probably account for the results of Figure 3e,f. To summarize the results from Figures 2 and 3, it is believed that some regularities exist: the initial driving force for CE is induced by curvature differences under the contact-separation mode (smaller applied forces), in which

DOI: 10.1021/acsnano.8b08533
ACS Nano XXXX, XXX, XXX–XXX

a surface of larger curvature obtains negative charges more easily. Increasing the applied force is likely to result in irregular surface deformations and surface damage or even material transfer due to relative sliding. All these complicate the predictability of the direction of charge transfer.

Among the influential factors of CE, temperature is a crucial element aside from applied force.[33,34] Since the surfaces of PTFE used in TENGs are likely to be changed/damaged at a temperature of 353 K or above,[35] Kapton with better heat stability is adopted as the tribomaterial to prepare the TENG in this study. Moreover, since the increase of temperature leads to dramatic changes in humidity in the environment, a vacuum and high-temperature testing platform is designed and shown in Figure 4a. This platform can provide relatively low vacuum (~1 Pa) to exclude humidity effects in high-temperature measurements. Figure 4b,c are the results of V_{OC} and Q_{SC} obtained from the TENG with a convex surface and a flat surface under a temperature from 298 to 358 K. The charge transfer under vacuum and high temperature is in accordance with the results in Figures 2 and 3, which is that convex Kapton films of larger curvature are prone to be negatively charged. Additionally, V_{OC} and Q_{SC} are 0.6 V and 0.25 nC under vacuum and 298 K, three times larger than those under atmospheric pressure and at the same temperature (Figure S5). The relative humidity under vacuum in this experiment is far lower than 1%, indicating the reduction of water in the air benefits the increase of charge transfer in CE. This notion is in contrast to previous studies on ions generated from the water in humid air being the primary medium of charge transfer in CE.[36] Therefore, it is possible to exclude the ion transfer mechanism of water as the basis for charge transfer in CE between identical materials. Additionally, the increase of temperature results in the decrease of electrification, as shown in Figure 4b,c. Since high temperature may change the surface nature of polymer films and decrease the electrification in effect, we retested the TENG three times with repetitively increasing and decreasing the temperature. It shows that the quantity of electrification can return to the original level following surface changes at high temperature, suggesting that the decrease in electrification is not attributed to film surface damage but lies in the deleterious effect of high temperatures. This is consistent with previous results that the CE between two different materials always decreased with a temperature increase, which could be partly attributed to the thermionic electron emission.[7,25,33,37] Figure 4d,e shows the V_{OC} and Q_{SC} obtained from the TENG with two flat Kapton films as the temperature increases from 298 K to 388 K. It is found that the V_{OC} and Q_{SC} under vacuum and 298 K also reach 3 times those under ambient pressure and at the same temperature (Figure S9). The same decrease of electrification also occurs with an increase of temperature. With temperature increases to 358 K then decreases to 298 K, the V_{OC} and Q_{SC} remain the same as those in Figure 4b,c. But provided that the temperature further increases to 388 K and then drops to 298 K, both the V_{OC} and Q_{SC} decrease (Figure 4f). Scanning electron microscopy (SEM) images (Figure 4g–i) indicate that the Kapton surface of the TENG at 358 K exhibits some minor impressions after contact, probably due to the softened surface at high temperatures. Conversely, many defects and damage of different sizes emerge on the Kapton surface at 388 K (Figure 4i, Figure S10), which may be the predominant reason for degradation in TENG performance after returning back to room temperature. All of the aforementioned results reveal that despite the increase of temperature decreasing the electrification, temperature is not a determining factor in the direction of charge transfer in CE between identical materials, echoing the findings of Lowel *et al.*[13]

Based on the above experimental results, a surface states model is proposed to explain the mechanism of CE between identical materials in Figure 5. When two ideal flat surfaces

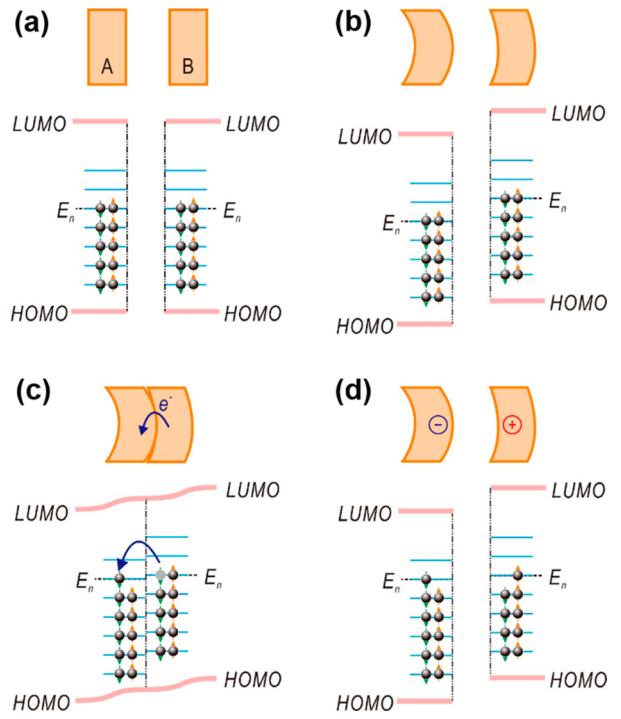

Figure 5. Mechanism of CE between identical materials. (a) Surface states model of the identical materials A and B with ideal flat surfaces. (b–d) Charge transfer before contact, in contact, and after contact between the identical materials A and B with different surface curvatures (depicted by orange shapes) explained by the surface states models. LUMO, lowest unoccupied molecular orbital; E_n, neutral level of surface states; HOMO, highest occupied molecular orbital.

composed of chemically identical materials A and B contact each other, no electron transfer occurs in that the neutral levels of surface states (E_n) are equivalent and horizontally matched (Figure 5a). However, CE emerges even when two flat surfaces mutually contact each other in the present experiment. This is probably due to the fact that flat surfaces are less likely to be absolutely smooth at the nano-microscale, and curvature differences determine the direction of charge transfer in terms of microstructures. Figure 5b–d show charge transfer before contact, in contact, and after contact between two identical materials A and B with different surface curvatures, within which there is a convex surface in A (*i.e.*, larger curvature) and a concave surface in B (*i.e.*, smaller curvature). The curvature difference may result in different surface energy, which may lead to a shift of surface states E_n. As shown in Figure 5b, the E_n shifts to a lower level for the convex surface, whereas it shifts to a higher level for the concave surface than that of flat surfaces in Figure 5a. When the two convex and concave surfaces contact each other (Figure 5c), electrons located at high-energy states in B will transfer to the low-energy states of the surface states of A. To some extent, this is a similar concept to that of charge density in conductors being

DOI: 10.1021/acsnano.8b08533
ACS Nano XXXX, XXX, XXX–XXX

greater at regions of large curvature and lower in small curvature regions.[38] In other words, the contact position on surfaces of large curvature can accommodate more electrons than that on small curvature surfaces when in contact, resulting in the flow of electrons from the latter to the former. Figure 5d shows that the separation between the two identical materials results in negative charges on A and an equivalent amount of positive charges on B. Even though the research findings are obtained on the macrosurfaces, it may well be available on microsurfaces on considering the relationship between CE and micro/nanostructures of surfaces,[39] which certainly needs to be further validated using other techniques such as atomic force microscopy (AFM). It is worth noting that the prerequisite for the above mechanism is the utilization of a contact-separation mode with a gently applied force that is not expected to cause surface damage. In addition, the micro/nanosurface roughness may change and the local stain/stress generated in the films may vary, according to the curvature difference. Both of these are likely to influence the direction of charge transfer, which still needs further study.

CONCLUSION

In summary, we introduce the same material made TENG to investigate the CE between identical materials. The results show no apparent tendency of the direction of charge transfer between two flat films. However, for the curved surface to be contacted, the films with a convex surface (larger curvature) are prone to be negatively charged, while the films with a concave surface (smaller curvature) are inclined to be positively charged. The performance of the TENG with surfaces of different positive curvatures also suggests that larger curvature leads to more electrons negatively charging the surface. In addition, an increase of applied force is likely to lead to a reversal of charge transfer direction between the two surfaces. Further verification on the above-mentioned charge trends between identical materials is conducted under a vacuum of ∼1 Pa and at a temperature as high as 358 K. On the basis of these experimental results, we propose a curvature-dependent charge transfer model for CE by introducing the curvature-induced energy shifts of the surface states. The prerequisite for the above model is the utilization of a contact-separation mode with a gentle applied force, since increasing the force is likely to result in irregular surface deformations and surface damage or even material transfer due to relative sliding. All of these complicate the predictability of the charge transfer direction. Our study may provide a possibility for the unification of the mechanisms of CE between different materials and between the identical materials in the future.

EXPERIMENTAL SECTION

Fabrication of the TENG. PTFE film with a thickness of 0.05 cm^{-1}, FEP film with a thickness of 0.025 cm^{-1}, Kapton film with a thickness of 0.025 cm^{-1}, polyester film with a thickness of 0.025 cm^{-1}, Nylon film with a thickness of 0.05 cm^{-1}, and acrylic sheets with different curvatures were purchased from McMaster-Carr. For the preparation of the TENG, a Cu coating with a thickness of 200 nm was deposited on the back of each tribomaterial film as the electrode by using a Denton Explorer e-beam evaporator. Then, the films with a Cu coating were bonded to the acrylic sheet with different curvatures by Kapton tape. Two of these acrylic sheets with the same tribomaterial film constituting the TENG and Ni wires were connected to each of the Cu electrodes for measurement. The structure of the TENG is shown in Figure S1a. The surface area of the tribomaterial film of each surface used in the TENG was about 8 cm^2.

Measurement of the TENG. For TENGs operated in ambient air, the temperature was controlled at 298 K and the relative humidity was less than 50%. For TENGs operated at high temperature, a vacuum assessment platform contained in a chamber was designed (Figure 4a). The chamber was mainly equipped with a heater, which provided the desired temperature with an accuracy of ±2 K, a mechanical feedthrough with a steel rod, and a vacuum system. The pressure was about 1 Pa^{-1} and the relative humidity was less than 1% in the chamber. Nickel wires were attached to the Cu electrodes and extended out of the chamber. The steel rod was connected with a linear motor, which provided an accurate control of position and speed for the mechanical stimulation. The separation distance between the two tribomaterial surfaces of the TENG was 1 cm. To eliminate the initial charges, the discharge treatment was carried out in two processes. First, once the TENG was prepared, both the acrylic substrates and tribomaterial films were rinsed with anhydrous ethanol and 2-propanol three times and then dried in ambient air for 48 h, respectively. Second, before each measurement, the surface of the tribomaterial film was rinsed with anhydrous ethanol three times and then dried in ambient air for at least 8 h. The open-circuit voltage V_{OC} and short-circuit transfer charge Q_{SC} of the TENG were measured by a Keithley 6514 electrometer. The relative humidity was measured by a Shaw Superdew 3 hygrometer. The forces applied to the TENG were measured by a Vernier LabQuest Mini force dynamometer. The microscope images of the surface of Kapton films were measured by a Hitachi SU8010 field-emission SEM.

ASSOCIATED CONTENT

Supporting Information

The Supporting Information is available free of charge on the ACS Publications website at DOI: 10.1021/acsnano.8b08533.

Properties of the PTFE TENG with many initial surface charges, V_{OC} and Q_{SC} of the PTFE TENG when the contact position is kept the same each time, properties of the FEP TENG, Kapton TENG, polyester TENG, and nylon TENG, V_{OC} and Q_{SC} of the PTFE TENG with different surface curvatures, properties of the Kapton TENG under atmospheric pressure and at room temperature, SEM images of the Kapton surface (PDF)

AUTHOR INFORMATION

Corresponding Author

*E-mail: zhong.wang@mse.gatech.edu (Z.-L. Wang).

ORCID

Zhiqun Lin: 0000-0003-3158-9340

Zhong Lin Wang: 0000-0002-5530-0380

Author Contributions

‖C. Xu, B. Zhang, and A. C. Wang contributed equally to this work.

Notes

The authors declare no competing financial interest.

ACKNOWLEDGMENTS

The authors are grateful for the support received from Hightower Chair Foundation. C.X. thanks the Outstanding Teacher Overseas Research Project of China University of Mining and Technology.

REFERENCES

(1) Lowell, J. Contact Electrification of Metals. *J. Phys. D: Appl. Phys.* **1975**, *8*, 53−63.

(2) Harper, W. R. The Volta Effect as a Cause of Static Electrification. *Proc. R. Soc. A* **1951**, *205*, 83−103.

DOI: 10.1021/acsnano.8b08533
ACS Nano XXXX, XXX, XXX−XXX

(3) Hays, D. A. Contact Electrification between Mercury and Polyethylene: Effect of Surface Oxidation. *J. Chem. Phys.* **1974**, *61*, 1455−1462.
(4) Lowell, J. Surface States and the Contact Electrification of Polymers. *J. Phys. D: Appl. Phys.* **1977**, *10*, 65−71.
(5) Liu, C.; Bard, A. J. Electrons on Dielectrics and Contact Electrification. *Chem. Phys. Lett.* **2009**, *480*, 145−156.
(6) Zhou, Y. S.; Wang, S.; Yang, Y.; Zhu, G.; Niu, S.; Lin, Z.-H.; Liu, Y.; Wang, Z. L. Manipulating Nanoscale Contact Electrification by an Applied Electric Field. *Nano Lett.* **2014**, *14*, 1567−1572.
(7) Xu, C.; Zi, Y.; Wang, A. C.; Zou, H.; Dai, Y.; He, X.; Wang, P.; Wang, Y.; Feng, P.; Li, D.; et al. On the Electron-Transfer Mechanism in the Contact-Electrification Effect. *Adv. Mater.* **2018**, *30*, 1706790.
(8) Gilbert, J. S.; Lane, S. J.; Sparks, R. S. J.; Koyaguchi, T. Charge Measurement on Particle Fallout from a Volcanic Plume. *Nature* **1991**, *349*, 598−600.
(9) Stow, C. D. Dust and Sand Storm Electrification. *Weather* **1969**, *24*, 134−137.
(10) Eden, H. F.; Vonnegut, B. Electrical Breakdown Caused by Dust Motion in Low-Pressure Atmospheres: Considerations for Mars. *Science* **1973**, *180*, 962−963.
(11) Boland, D.; Al-Salim, Q. A. W.; Geldart, D. Static Electrification in Fluidized Beds. *Chem. Eng. Sci.* **1969**, *24*, 1389−1390.
(12) Henry, P. S. H. The Role of Asymmetric Rubbing in the Generation of Static Electricity. *Br. J. Appl. Phys.* **1953**, *2* (Suppl), S31−S36.
(13) Lowell, J.; Truscott, W. S. Triboelectrification of Identical Insulators: II. Theory and Further Experiments. *J. Phys. D: Appl. Phys.* **1986**, *19*, 1281−1298.
(14) Baytekin, H. T.; Patashinski, A. Z.; Branicki, M.; Baytekin, B.; Soh, S.; Grzybowski, B. A. The Mosaic of Surface Charge in Contact Electrification. *Science* **2011**, *333*, 308−312.
(15) Fan, F. R.; Tian, Z. Q.; Wang, Z. L. Flexible Triboelectric Generator. *Nano Energy* **2012**, *1*, 328−334.
(16) Zhang, S. L.; Lai, Y.; He, X.; Liu, R.; Zi, Y.; Wang, Z. L. Auxetic Foam-Based Contact-Mode Triboelectric Nanogenerator with Highly Sensitive Self-Powered Strain Sensing Capabilities to Monitor Human Body Movement. *Adv. Funct. Mater.* **2017**, *27*, 1606695.
(17) Wen, Z.; Shen, Q.; Sun, X. Nanogenerators for Self-Powered Gas Sensing. *Nano-Micro Lett.* **2017**, *9*, 45.
(18) Zi, Y.; Niu, S.; Wang, J.; Wen, Z.; Tang, W.; Wang, Z. L. Standards and Figure-of-Merits for Quantifying the Performance of Triboelectric Nanogenerators. *Nat. Commun.* **2015**, *6*, 8376.
(19) Wang, Z. L.; Jiang, T.; Xu, L. Toward the Blue Energy Dream by Triboelectric Nanogenerator Networks. *Nano Energy* **2017**, *39*, 9−23.
(20) Wang, P.; Liu, R.; Ding, W.; Zhang, P.; Pan, L.; Dai, G.; Zou, H.; Dong, K.; Xu, C.; Wang, Z. L. Complementary Electromagnetic-Triboelectric Active Sensor for Detecting Multiple Mechanical Triggering. *Adv. Funct. Mater.* **2018**, *28*, 1705808.
(21) Zhang, S. L.; Xu, M.; Zhang, C.; Wang, Y.; Zou, H.; He, X.; Wang, Z.; Wang, Z. L. Rationally Designed Sea Snake Structure Based Triboelectric Nanogenerators for Effectively and Efficiently Harvesting Ocean Wave Energy with Minimized Water Screening Effect. *Nano Energy* **2018**, *48*, 421−429.
(22) Chen, X. Y.; Wu, Y. L.; Yu, A. F.; Xu, L.; Zheng, L.; Liu, Y. S.; Li, H. X.; Wang, Z. L. Self-Powered Modulation of Elastomeric Optical Grating by Using Triboelectric Nanogenerator. *Nano Energy* **2017**, *38*, 91−100.
(23) Niu, S. M.; Liu, Y.; Chen, X. Y.; Wang, S. H.; Zhou, Y. S.; Lin, L.; Xie, Y. N.; Wang, Z. L. Theory of Freestanding Triboelectric Layer-Based Nanogenerators. *Nano Energy* **2015**, *12*, 760−774.
(24) Willatzen, M.; Wang, Z. L. Theory of Contact Electrification: Optical Transitions in Two-Level Systems. *Nano Energy* **2018**, *52*, 517−523.
(25) Xu, C.; Wang, A. C.; Zou, H.; Zhang, B.; Zhang, C.; Zi, Y.; Pan, L.; Wang, P.; Feng, P.; Lin, Z.; et al. Raising the Working Temperature of a Triboelectric Nanogenerator by Quenching Down Electron Thermionic Emission in Contact-Electrification. *Adv. Mater.* **2018**, *30*, 1803968.
(26) Wei, X. Y.; Zhu, G.; Wang, Z. L. Surface-Charge Engineering for High-Performance Triboelectric Nanogenerator Based on Identical Electrification Materials. *Nano Energy* **2014**, *10*, 83−89.
(27) Apodaca, M. M.; Wesson, P. J.; Bishop, K. J. M.; Ratner, M. A.; Grzybowski, B. A. Contact Electrification between Identical Materials. *Angew. Chem., Int. Ed.* **2010**, *49*, 946−949.
(28) Inculet, I. I.; Castle, G. S. P.; Aartsen, G. Generation of Bipolar Electric Fields during Industrial Handling of Powders. *Chem. Eng. Sci.* **2006**, *61*, 2249−2253.
(29) Zhao, H.; Castle, G. S. P.; Inculet, I. I. The Measurement of Bipolar Charge in Polydisperse Powders Using a Vertical Array of Faraday Pail Sensors. *J. Electrost.* **2002**, *55*, 261−278.
(30) Forward, K. M.; Lacks, D. J.; Sankaran, R. M. Charge Segregation Depends on Particle Size in Triboelectrically Charged Granular Materials. *Phys. Rev. Lett.* **2009**, *102*, 028001.
(31) Lin, L.; Xie, Y.; Wang, S.; Wu, W.; Niu, S.; Wen, X.; Wang, Z. L. Triboelectric Active Sensor Array for Self-Powered Static and Dynamic Pressure Detection and Tactile Imaging. *ACS Nano* **2013**, *7*, 8266−8274.
(32) Dai, K.; Wang, X.; Yi, F.; Jiang, C.; Li, R.; You, Z. Triboelectric Nanogenerators as Self-Powered Acceleration Sensor under High-G Impact. *Nano Energy* **2018**, *45*, 84−93.
(33) Zhao, Z.; Pu, X.; Du, C.; Li, L.; Jiang, C.; Hu, W.; Wang, Z. L. Freestanding Flag-Type Triboelectric Nanogenerator for Harvesting High-Altitude Wind Energy from Arbitrary Directions. *ACS Nano* **2016**, *10*, 1780−1787.
(34) Wen, X.; Su, Y.; Yang, Y.; Zhang, H.; Wang, Z. L. Applicability of Triboelectric Generator over a Wide Range of Temperature. *Nano Energy* **2014**, *4*, 150−156.
(35) Lu, C. X.; Han, C. B.; Gu, G. Q.; Chen, J.; Yang, Z. W.; Jiang, T.; He, C.; Wang, Z. L. Temperature Effect on Performance of Triboelectric Nanogenerator. *Adv. Eng. Mater.* **2017**, *19*, 1700275.
(36) Naik, S.; Mukherjee, R.; Chaudhuri, B. Triboelectrification: A Review of Experimental and Mechanistic Modeling Approaches with a Special Focus on Pharmaceutical Powders. *Int. J. Pharm.* **2016**, *510*, 375−385.
(37) Yang, Y.; Zhou, Y.; Wu, J. M.; Wang, Z. L. Single Micro/Nanowire Pyroelectric Nanogenerators as Self-Powered Temperature Sensors. *ACS Nano* **2012**, *6*, 8456−8461.
(38) Liu, K. Relation between Charge Density and Curvature of Surface of Charged Conductor. *Am. J. Phys.* **1987**, *55*, 849−852.
(39) Wang, A. E.; Gil, P. S.; Holonga, M.; Yavuz, Z.; Baytekin, H. T.; Sankaran, R. M.; Lacks, D. J. Dependence of Triboelectric Charging Behavior on Material Microstructure. *Phys. Rev. Mater.* **2017**, *1*, 035605.

DOI: 10.1021/acsnano.8b08533
ACS Nano XXXX, XXX, XXX−XXX